Pergamon

Int. Comm. Heat Mass Transfer, Vol. 24, No. 2, pp. 285–294, 1997

0735-1933/97 $17.00 + .00

PII S0735-1933(97)00014-6

CROSS-DUCT ELECTRIC FIELD PERTURBATION VOID FRACTION PROBE

D. Duncan and T.A. Trabold
Lockheed Martin Corporation
P.O. Box 1072
Schenectady, New York 12301

(Communicated by J.P. Hartnett and W.J. Minkowycz)

ABSTRACT

An advanced probe has been developed for transient and time-averaged measurement of the void fraction under various thermal-hydraulic conditions. The Electric Field Perturbation (EFP) probe operates by measuring the electrical properties of a two-phase mixture which are related to the void fraction by a theoretical electromagnetic field model. Qualification tests were performed in both air-water and high pressure steam-water facilities. In the former set of experiments, the EFP measurements were compared to void fractions obtained with fast-acting valves and a hot-film anemometer. For high-pressure experiments in a pool boiling configuration, simultaneous void fraction time traces from the EFP probe and differential pressure cell indicated that the EFP probe responds well to overall void fraction fluctuations.

Introduction

There is presently a great deal of interest in acquiring fundamental understanding of various two-phase flow phenomena, with the ultimate objective of improving thermal-hydraulic predictive methods. Due to the complicated geometries and extreme flow conditions associated with thermal-hydraulic testing, significant efforts have been directed toward development of advanced two-phase flow instrumentation. Of the various parameters that need to be measured, the local void fraction is of primary interest for defining the two-phase flow environment.

Electrical instrumentation techniques are particularly attractive for local void fraction measurements, due to their ability to resolve high frequency changes in the two-phase flow field. The general principle of operation of electrical void fraction probes is based on the difference in the electrical properties between the liquid and vapor phases, and has been described in detail elsewhere [1,2]. General problems encountered with electrical sensors include phase distortion, electrochemical effects, nonrepresentative conductive paths, nonlinear response due to the effect of flow regime, probe wetability and surface tension. To minimize these problems, it is required that the sensor and measurement technique be designed and calibrated specifically for the desired

measurement. Also, most instruments lose their sensitivity when the sensing device is positioned at a significant distance from the data acquisition hardware or when there is a change in the electrical properties of the fluid. This is primarily due to either the increase in the signal-to-noise ratio caused by increasing the length of the transmission cable, or significant changes in dielectric constant or resistance of the fluid, both of which decrease the ability to resolve the signal.

A new proprietary electrical method which overcomes these deficiencies, hereafter referred to as the Electric Field Perturbation (EFP) technique, has been developed by Mohr and Associates[1]. Based on this technique, various probe designs for specific applications have been developed jointly by the Lockheed Martin Corporation and Mohr and Associates. The technique is based on using the perturbation to an electric field to indicate the relative changes in void fraction. As illustrated in Figure 1, EFP probes of three different configurations have been designed for testing in cross-duct, tube bundle and pool boiling applications. The present report describes the results of extensive testing of the cross-duct EFP probe in atmospheric pressure air-water and high temperature steam-water flows. Investigation of the use of the EFP probe as a flow regime identification device is also discussed.

Air-Water Facility and EFP Probe Design

As a first step in the development of an EFP probe for thermal-hydraulic testing, it was considered essential to perform experiments in an air-water facility. These experiments enabled void fraction data to be acquired under easily controllable and measurable flow conditions, and provided a database for comparison with available experimental results. The flow loop, described in [3], consisted essentially of a magnetic drive pump, water tank with heater, air-water separator and several rotameters and pressure gauges for measurement of air and water flow rates.

As illustrated schematically in Figure 2, the test cell, 127 cm long and 6.35 × 0.64 cm in cross-section (D_H = 1.16 cm), was divided into two regions by three fast-acting valves (FAVs). All data were acquired in the lower test section half, between FAVs #1 and #2[2]. The distance from the test section inlet (below FAV#1) to the EFP probe measurement location was 78.74 cm, providing an effective hydrodynamic entrance length of $68D_H$. The acrylic test section halves were bolted to the FAVs using flanges and rubber gaskets. A novel feature of the test cell was that most of the 6.35 cm faces were comprised of removable acrylic windows into which the EFP probe components and other instrumentation were mounted. These windows, as well as all surfaces critical to the flow duct dimensions, were milled to size with a tolerance of ±0.1 mm. By bolting the windows into openings provided in the test cell body and using vacuum grease as the sealant material, smooth and watertight internal test section flow paths were created. The fast-acting valves provided a means of measuring volume-average void fraction by rapidly (in about 0.1 sec) closing and trapping the two-phase mixture. The gas then migrates to the top of the trapped space

1. An engineering and consulting firm located in Richland, WA
2. The upper half of the test cell was used for simultaneous tube bundle EFP probe experiments.

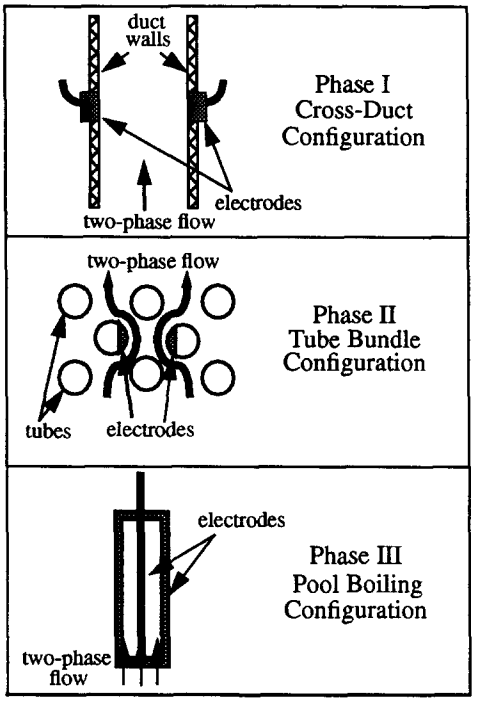

FIG. 1
Three EFP Probe Designs

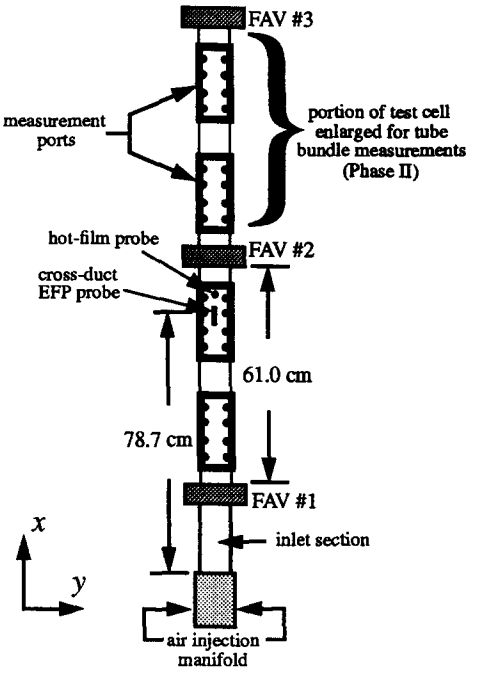

FIG.2
Air-Water Test Cell

and the average volumetric void fraction ($\overline{\alpha}$) may be determined by the relative heights of the two phases.

In order to provide a wide variety of two-phase flow conditions under which to test the EFP probe performance, two air injection schemes were employed. The first consisted of two 2.54 cm ID PVC air lines connected to the transition piece (containing layers of screens and tubes to flatten the velocity profile) between the diverging section and the test section inlet spool piece immediately upstream of FAV #1. This scheme generally produced a relatively small number of large bubbles (approximately 2 to 8 mm mean diameter) at low air flow rates. The second air injection method consisted of a porous "soapstone" material contained in an annular arrangement within a plexiglas cylinder. This assembly was connected in-line with the water inlet introduced at the bottom of the vertical test section. The flow of water through the cylinder acted to shear off air bubbles as they emanated from the surface of the soapstone, thereby creating a relatively large number of small bubbles. For all experiments, a small amount of liquid soap was added to the water to lower the surface tension.

For application in the air-water loop, the low pressures and temperatures made the EFP

probe design relatively simple. This design has been optimized using a finite element electromagnetic code. By assuming that the voids were homogeneously distributed in the dielectric space, a functional form for the void fraction versus the relative impedance of the medium was obtained. This functions' endpoints were fixed by measurements in 100% air and 100% water. The function was then corrected for the known temperature dependence of the dielectric constant. This functional form was used subsequently in all air-water and steam-water measurements.

The probe design and materials influence the output signal and therefore require different signal-to-void fraction data analysis algorithms. Different designs using various dielectric materials and fabrication procedures were conceived, keeping in mind the ultimate high pressure and temperature application. To date, several potential designs have been developed. The final design, with the electrodes imbedded in low temperature dielectric blocks, was used during feasibility testing in the air-water test loop and in high pressure tests. These units were fabricated to be mounted within the acrylic windows which fit into the transverse faces of the air-water test cell (Figure 2). The electrical lines were brought out through pressure seals and connected to each other and ultimately to the data acquisition system. An EFP probe of similar configuration was fabricated for the high pressure cell using a metal mounting block to hold the dielectric material blocks at a constant spacing of 0.64 cm. In this case, the electrical connections had to be made inside the high pressure chamber. Since the available off-the-shelf electrical components were limited in temperature capability, tests were performed only up to about 180 °C. More details on the EFP probe fabrication are available in [3].

Results and Discussion

Air-Water Tests

The general approach used in air-water tests was to acquire EFP probe, hot-film anemometry and fast-acting valve data over wide ranges of gas and liquid superficial velocities, in order to rigorously evaluate the EFP probe performance under various two-phase flow conditions. The test section chosen for these experiments is a geometry often tested for high temperature thermal-hydraulic studies. Jones and Zuber [4] have reported local void fraction measurements across the 5 mm dimension of a high aspect ratio duct, the geometry of which is quite similar to that of the present test section. These data provided a means of confirming the present hot-film anemometry results, and aided in the validation of EFP probe void fraction measurements.

In order to confirm the operation of the fast-acting valves, the volume-average void fraction data thus obtained were reduced in terms of the mean gas phase velocity ($j_g/\bar{\alpha}$). These data showed close agreement to the drift flux equation fit by Wallis [5] of slug rise velocity data from Griffith [6], with the distribution parameter computed by the relation of Ishii [7]. The volume average void fractions obtained using the fast-acting valve technique do not, however, provide an absolute standard for EFP probe qualification. The gas phase distributions across the transverse and thickness test section dimensions are affected by so many factors (e.g., flow regime, air injection method, entrance length) that development of a general relationship between $\bar{\alpha}$ and the local

void fraction is impractical. In order to acquire local void fraction data which would provide a more precise basis for evaluation of the EFP probe void fraction measurements, a conical hot-film anemometer probe was installed, such that the sensitive portion at the probe tip was located 1.3 cm downstream of the upper edge of the EFP probe. The constant temperature hot-film anemometer (HFA) consisted essentially of a probe which is directly exposed to the two-phase flow field, and electronic circuitry which controlled the amount of current supplied to the probe. A FORTRAN program based on that developed by Lee [8] was used to process the HFA voltage data. The use of the HFA technique for measurement of local void fraction has been sufficiently treated elsewhere [3,4] and will not be repeated here. The method has been confirmed previously by comparison to line-average void fractions obtained with a gamma densitometer [9].

Since for duct flow applications, the EFP probe electrodes are placed on opposite sides of the test section (Figure 1), the resulting void fraction measurements are essentially line-averages. In order to obtain line-average data from the present HFA results, the assumption was made that the void distributions follow power law profiles

$$\alpha = \alpha_{max}[1-\eta^b] \tag{1}$$

where η and b are the dimensionless distance from the duct centerline and the power law exponent, respectively. The line-average void fraction is then calculated by integrating Equation 1 to yield

$$\bar{\alpha} = \left(\frac{b}{b+1}\right)\alpha_{max} \tag{2}$$

where α_{max} is assumed to be the measured centerline void fraction. To calculate the line-average void fraction from the present HFA data, power law exponents were extracted from Figure 10 of Jones and Zuber [4]. The approach was validated by comparing centerline and off-centerline data presented in [4] with the present results, an example of which is shown in Figure 3. Differences between the values of gas and liquid flowrates tested in [4] and in the present experiments

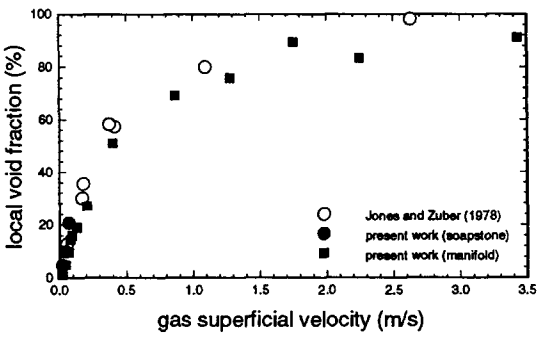

FIG. 3
Comparison of Present Center-Line Void Fraction Data ($j_l = 0.64$ m/s) with Results of Jones and Zuber [4] ($j_l = 0.61$ m/s)

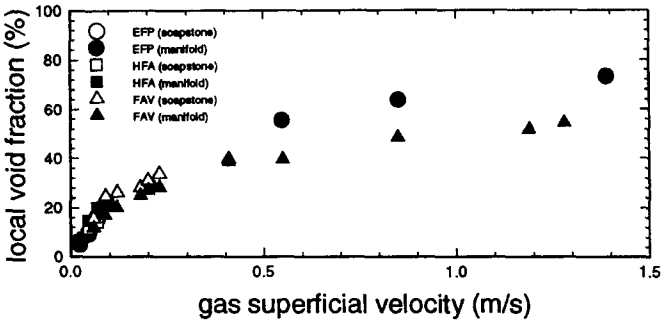

FIG. 4
Comparison of Average Void Fraction Data for $j_l = 0.22$ m/s

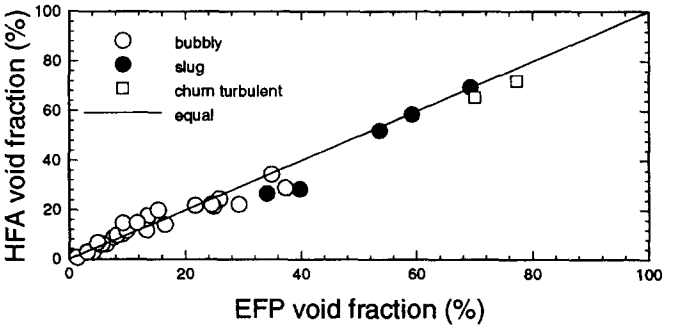

FIG. 5
Comparison of EFP and HFA Measurements

were accounted for by interpolation between data points in the former. For 21 of the 33 flow conditions reported here, the value of the power law exponent fell in the range $1.60 < b \leq 1.85$. At higher average void fractions, the power law exponent approached 4.0.

Comparison of void fraction results from cross-duct Electric Field Perturbation probe and HFA and FAV instrumentation is illustrated in Figures 4 and 5. In the former figure, the line-average EFP void fraction measurements are compared to line-average and volume-average data acquired with the hot-film anemometer and fast-acting valves, respectively, as a function of air flow rate for a single liquid mass flux. As expected, the trends are similar in functional form but the EFP and HFA probes yielded appreciably higher void fraction measurements than the fast-acting valves beyond the bubbly flow regime, since these instruments were positioned at the center of the transverse (y) duct dimension (Figure 2). As mentioned, the best basis of evaluation of the EFP void fraction measurement is provided by the centerline hot-film anemometry data which are corrected to line-averages. In Figure 5 a direct comparison between these measurements is provided. In general, the agreement between the two data sets is quite good for the entire range of

void fraction up to about 80%[1]. The average difference between concomitant measurements for all 32 points in Figure 5 is 2.8% in void fraction. It appears, however, that the degree of correspondence between the HFA and EFP data depends on flow regime. Among the bubbly flow data, the average deviation is 1.7% void fraction. The slug flow data has an average difference between EFP and HFA results of 4.4%. It appears that the most significant deviations occur in the range $30 \leq \bar{\alpha} \leq 40\%$, where low frequency air slugs dominate the two-phase flow field. This flow regime contributes to two primary sources of error. First, the assumption of a homogeneous void volume in the EFP probe computational model is clearly not met in this regime and therefore, the correlation between relative impedance and void fraction is not directly applicable. Second, the time-averaging period used in the measurement of void fraction was different between the two instruments. The HFA results were based on voltage data acquired continuously at 10 kHz. Conversely, the EFP data were obtained by averaging 35 sets per second of 1024 samples acquired at a different high frequency. The EFP void fraction measurement is not continuous due to the small time required for writing each set of data to disk. Hence, variations in the measurement of average void fraction are to be expected in flows with low frequency periodicity. Although no data are presented for annular flow, it is expected that, for the same reasons as outlined above, a liquid film thickness related bias in the EFP measurement would exist.

As a first attempt at qualifying the cross-duct EFP probe for void fraction measurements, the results presented in this section were very encouraging. However, in order to further develop the EFP probe as a generally applicable instrument, it was clear that some account must be made for flow regime transitions and the significant differences in phase distribution among the regimes. As briefly discussed below, it is possible to use the EFP probe as a flow regime identification device. Once this determination is made, different theoretically derived correlations (for homogeneous, low frequency slug, annular flow) may then be automatically invoked. Since this approach in no way relies on an experimental standard, use of the same EFP probe in different applications may be facilitated by adjusting these correlations to account for flow geometry, fluid physical properties, etc. As discussed below, the same homogeneous correlation developed for air-water experiments was applied to pressurized steam-water measurements by simply taking into account the known variation of the fluid impedance with temperature.

High Temperature Steam-Water Tests

The high temperature steam-water tests were originally conceived to be a demonstration that the cross-duct EFP probe signal is readable at elevated temperature, and to provide some indication of the temperature dependence of the signal. The test results were obtained in a high pressure autoclave. This unit, 203 cm long and 7.4 cm ID, was fitted with several view ports, thermocouples and differential pressure (DP) cells. More details of this facility are provided in [3]. Although the steam-water tests were run only to a maximum temperature of about 180 °C, due to mechanical limitations of the solder used to fabricate the probe grounding connection, the output signal was found to vary in a measurable way with volume-average void fraction. A transient data plot,

1. The hot-film anemometer was not employed for $\bar{\alpha} \geq 80\%$ due to the potential for probe damage at air superficial velocities in excess of 3.5 m/s. However, the EFP probe was used in the annular flow regime, up to $\bar{\alpha} = 93.1\%$.

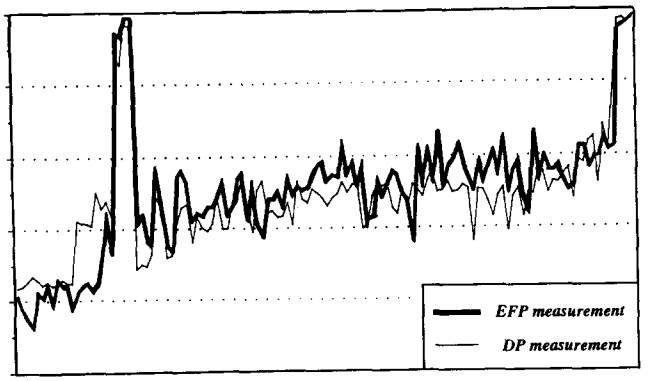

FIG. 6
Transient Steam-Water Void Fraction Data
(abscissa = 0 - 32 sec; ordinate = 0 - 100% void fraction)

illustrated in Figure 6, provides a comparison of the EFP and DP void fraction measurements. The EFP probe definitely responds to the gross variations in the flow, for example the steam "slug" in the first half of the data record. Although the transient trends are generally consistent, there is clearly a difference in the magnitudes of void fractions measured. Since the EFP probe is situated at the center of the autoclave, it is expected that it will yield a somewhat higher α than the volume-average value acquired with the DP transducer. In general, the results in Figure 6 were very encouraging since the correlation developed for air-water flows at atmospheric pressure was used to determine the void fraction based on EFP output signal. The only additions to the data analysis software were the known temperature variations of impedance for steam and water.

Flow Regime Identification Based on EFP Probe Signal

In any fundamental investigation of two-phase flow phenomena, identification of the flow regime is essential, since knowledge of the flow regime affords proper interpretation of experimental data. Also, for the purpose of multifluid modeling, flow regime transition criteria are needed to know under what flow conditions particular constitutive relations are applicable. Numerous studies published over the past fifty years have presented flow regime "maps", usually in terms of the gas and liquid superficial velocities or nondimensionless parameters based on these quantities. There are several problems with this approach. To date, no generally applicable criteria which account for fluid physical properties, duct geometry, pressure and temperature conditions and heating have been developed. Also, these maps are in almost all cases based on visual data which are subjective.

In the current test program, an attempt was made to ascertain the EFP probe's ability to identify the two-phase flow regimes, for two reasons. First, based on the results presented above for both air-water and steam-water systems, it appears that improvements in EFP probe accuracy are possible by first using it to determine the flow regime and then applying a regime-dependent (e.g., homogeneous, low frequency slug, annular) signal versus void fraction correlation. Second, for thermal-hydraulic testing at high temperature and pressure, a visual determination of the flow

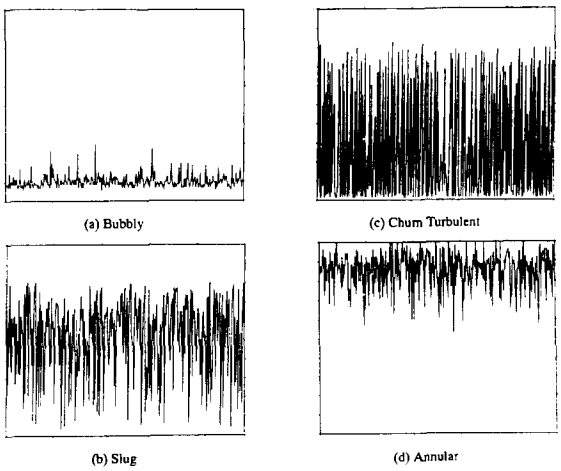

FIG. 7
Time Traces of Air-Water Void Fraction Data
(abscissa = 0 - 10 sec; ordinate = 0 - 100% void fraction)

regime is usually not possible. In these cases a nonintrusive, nonoptical device is the only means for flow regime identification.

Typical void fraction time traces for bubbly, slug, churn turbulent and annular air-water flows are illustrated in Figure 7. There is a variation with flow regime of both the magnitude and frequency of the void fraction fluctuations; bubbly and annular flows apparently possess less of the low frequency, high amplitude fluctuations visible in the slug and churn turbulent regimes. These characteristics indicate that statistical analysis in terms of the probability density function (PDF) or power spectral density (PSD) may be appropriate. Regardless of which type of analysis would provide the best vehicle for objective flow regime determination, a generally applicable approach would most likely involve a pattern recognition operation. This would enable automated conversion of the raw or transformed transient void fraction data to the associated flow regime, based on waveforms stored in a signal pattern database.

Concluding Remarks

Based on the tests discussed in the present report, it has been determined that the Electric Field Perturbation probe is a viable void fraction measurement technique for air-water and high temperature steam-water flows. It appears to be applicable over nearly the entire void fraction range and may be used to provide either transient or time-averaged void fraction measurements. This technique represents a significant advance in thermal-hydraulic instrumentation, for two reasons. First, the functional form of the signal versus void fraction relationship can be obtained by a theoretical electromagnetic field analysis. The only calibration needed is establishing the end

points of this function (0 and 100% void fraction), which can readily be accomplished in situ. Second, its application may, in principle, be extended to a wider temperature range and/or different fluids by incorporating the known gas and liquid dielectric properties into the data analysis software. To produce a probe for use in high temperature flows, the most significant remaining technical issue is the selection of appropriate materials and manufacturing techniques.

There are several steps which could be taken to improve the EFP probe accuracy. The probe could be applied first as a flow regime identification device, and then be used to measure the void fraction with a regime-dependent void distribution (e.g., homogeneous, low frequency slugs, annular flow) in the electromagnetic field code. Also, the EFP probe could be cross-qualified against simultaneous measurements with a gamma densitometer, by using the same time integration period and matching the gamma beam collimator size to that of the probe.

Nomenclature

b	exponent on power law void fraction distribution
D_H	hydraulic diameter
j_g, j_l	gas and liquid superficial velocity
α	local void fraction
$\overline{\alpha}$	line-average or volume-average void fraction
η	dimensionless distance from duct centerline

References

1. Hardy, J.E., and Hylton, J.O., *Int. J. Multiphase Flow, 10*, 541 (1984).

2. Duncan, D., Trabold, T.A., C.L. Mohr and M.K. Berrett, *Experimental Heat Transfer, Fluid Mechanics and Thermodynamics,* M.D. Kelleher *et al.* (Editors), 2, 1426, Elsevier Science Publishers B.V. (1993).

3. Duncan, D. and Trabold, T.A., U.S. Department of Energy Report KAPL-4780 (1996).

4. Jones, O.C. and Zuber, N., *AIChE Symposium Series, 74*, 191 (1978).

5. Wallis, G.B., *One-dimensional Two-phase Flow*, McGraw-Hill, New York (1969).

6. Griffith, P., *ASME J. Heat Transfer, 86*, 327 (1964).

7. Ishii, M., Argonne National Laboratory Report ANL-77-47 (1977).

8. Lee, S.J., M.S. Thesis, Rensselaer Polytechnic Institute, Troy, NY (1982).

9. Trabold, T.A., P.F., Moore, W.E., Morris, W.O., Symolon, P.D., Vassallo, P.F. and Kirouac, G.J., FED-Vol. 180, *Experimental and Computational Aspects of Validation of Multiphase CFD Codes*, ASME (1994).

Received July 8, 1996